Supplement of Atmos. Chem. Phys., 16, 1081–1104, 2016
http://www.atmos-chem-phys.net/16/1081/2016/
doi:10.5194/acp-16-1081-2016-supplement

Atmospheric Chemistry and Physics
Open Access
EGU

Supplement of

Size distribution and optical properties of mineral dust aerosols transported in the western Mediterranean

C. Denjean et al.

Correspondence to: C. Denjean (cyrielle.denjean@meteo.fr) and P. Formenti (paola.formenti@lisa.u-pec.fr)

Figure S1. Scattering cross section for the GRIMM 1.129 (red) and the FSSP-300 (blue) calculated from Mie theory as a function of nominal diameter. Calculations are shown for the refractive index of the standard spheres used for calibration ($\tilde{n}$ = 1.60-0.000i, dashed line) and typical dust refractive index ($\tilde{n}$ = 1.53-0.002i, line). The shadings indicate the nominal size ranges that were not considered for data analyses in this study due to flattering in the scattering cross section.

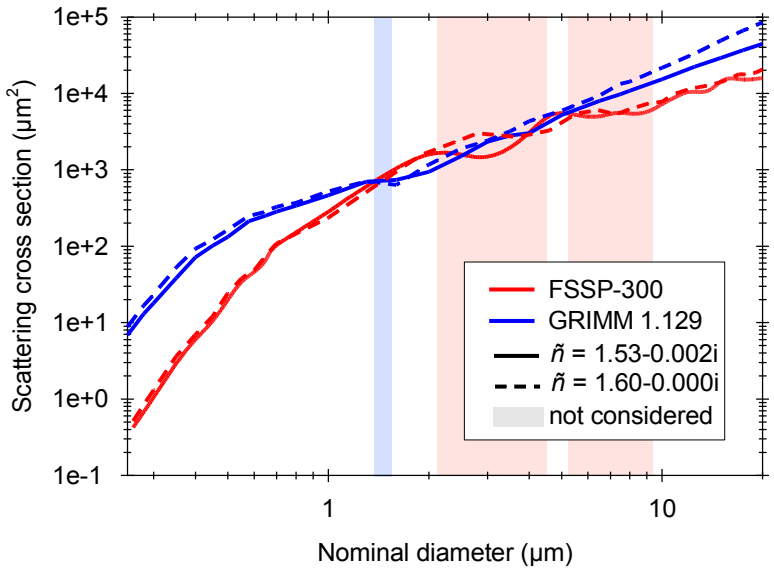

Figure S2. Particle size-dependent passing efficiency of the AVIRAD and CAI sampling inlets.

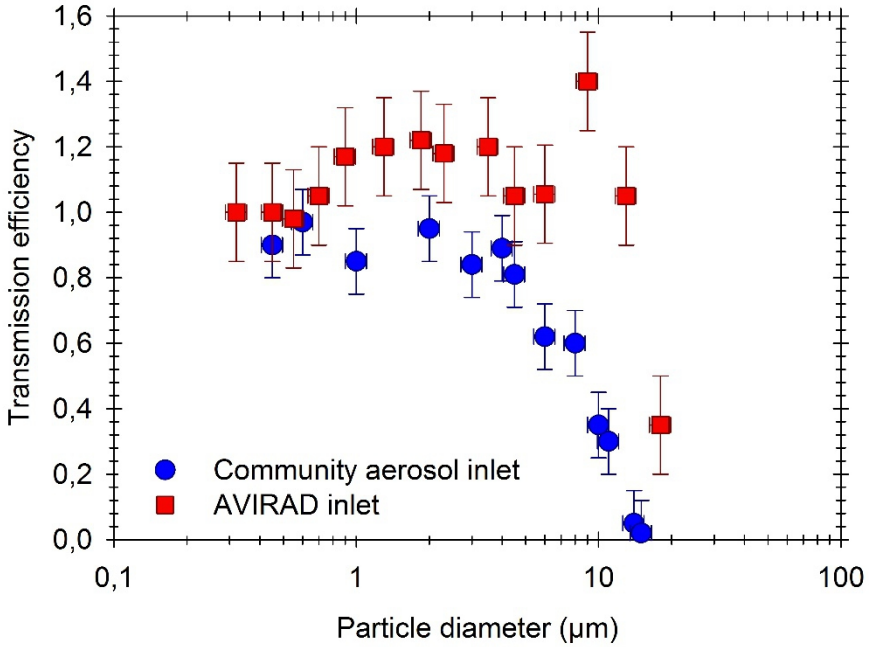

Figure S3. Mean sea level pressure (white labelled lines) and 500-hPa geopotential height (shaded contours) from the NCEP CFS Reanalysis at 12 UTC of 16 June 2013 (representative of the conditions encountered during F29 and F30), 17 June (during the flights F31 and F32), 19 June (F33), and 20 June (F34). Color scale from 476 to 600 geopotential decametres by step of 4.
Courtesy of http://www.wetterzentrale.de/topkarten/fscfsreaeur.html.

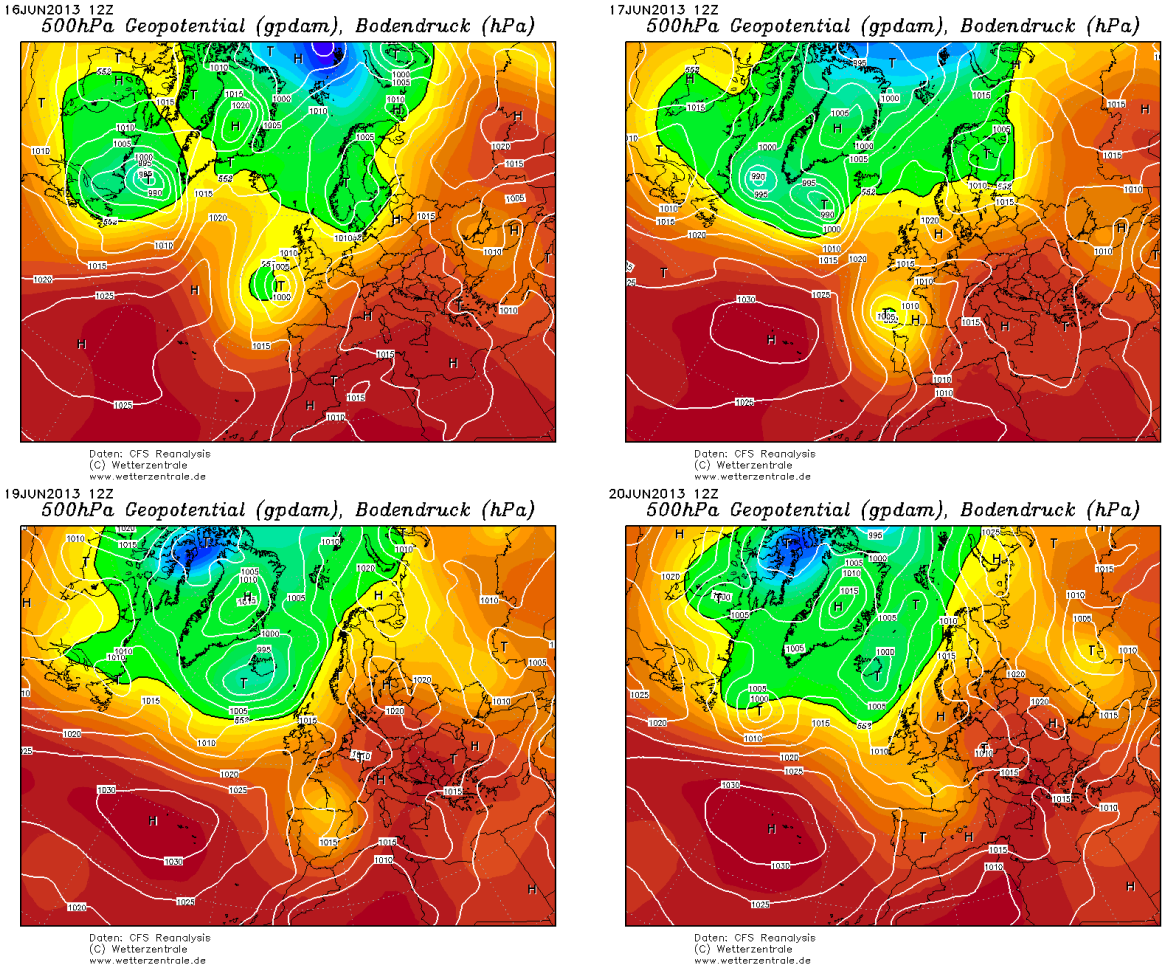

Figure S4. Mean sea level pressure (white labelled lines) and 500-hPa geopotential height (shaded contours) from the NCEP CFS Reanalysis at 12 UTC of 22 June 2013 (representative of the conditions encountered during F35 and F36), 28 June (during the flights F38 and F39), 02 July (F41), and 03 July (F42). Color scale from 476 to 600 geopotential decametres by step of 4.
Courtesy of http://www.wetterzentrale.de/topkarten/fscfsreaeur.html.

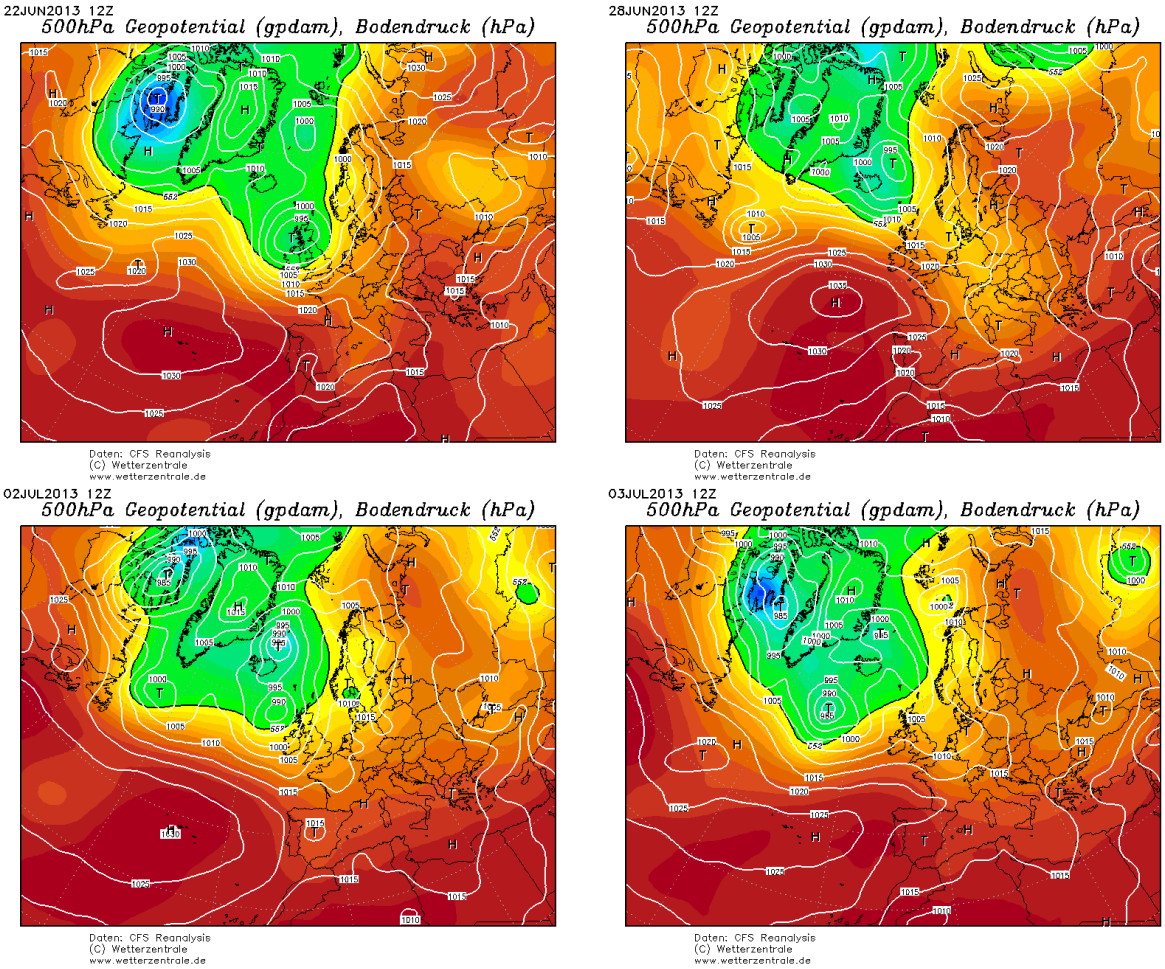

Figure S5. 700-hPa relative humidity (in %; shaded contours) and wind maps (half- and full-barb values for 5 and 10 m s^{-1}, respectively) from the 10-km resolution WRF model simulations. Valid times are 12 UTC of 17 June 2013, (flights F31-F32, top panel), 20 June (F34, middle) and 22 June (F35-F36, bottom).

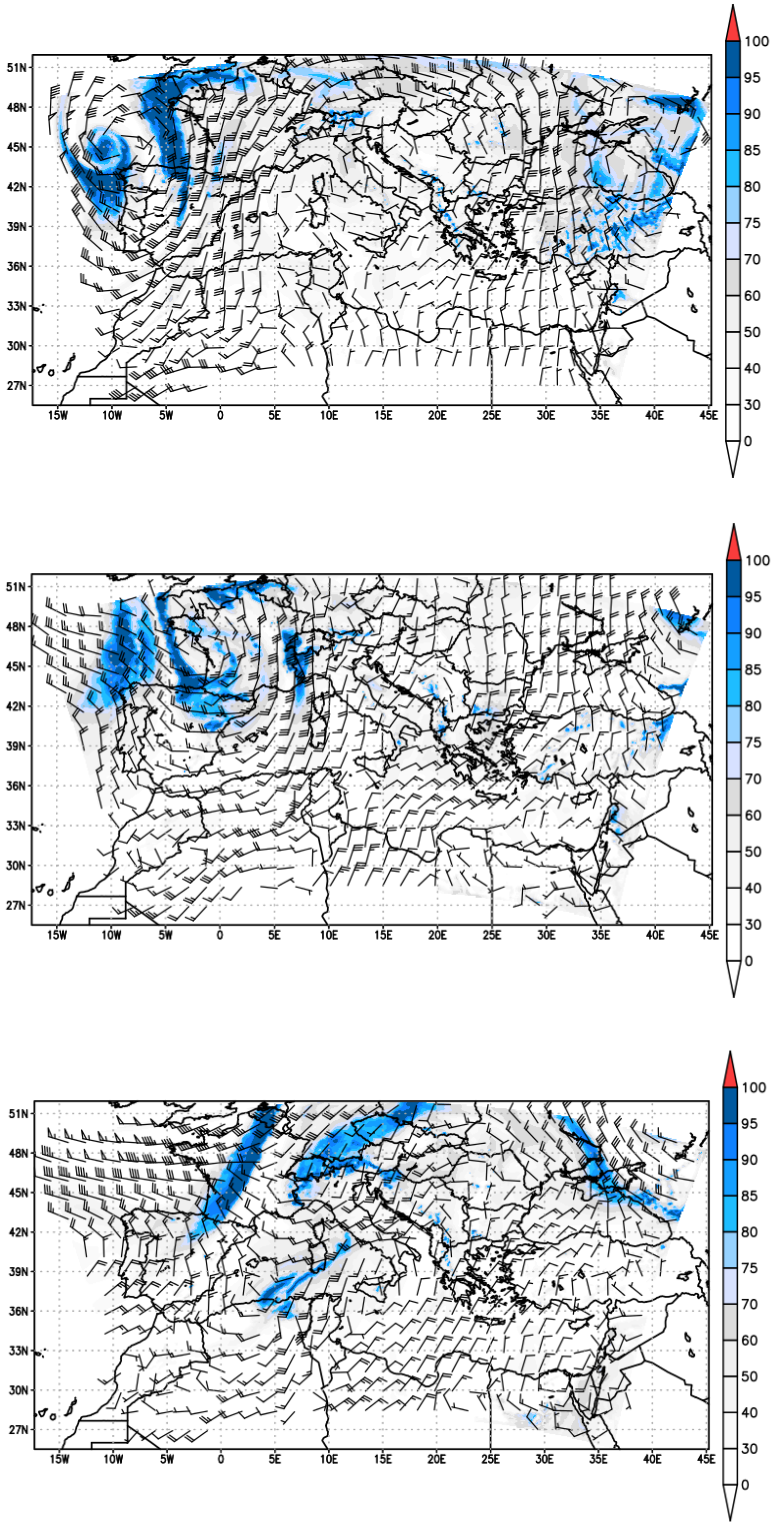

Figure S6. 700-hPa relative humidity (shaded contours) and wind maps from the 10-km resolution WRF model simulations. Valid times are 12 UTC of 28 June 2013, (flights F38-F39, top panel), 02 July (F41, middle) and 03 July (F42, bottom).

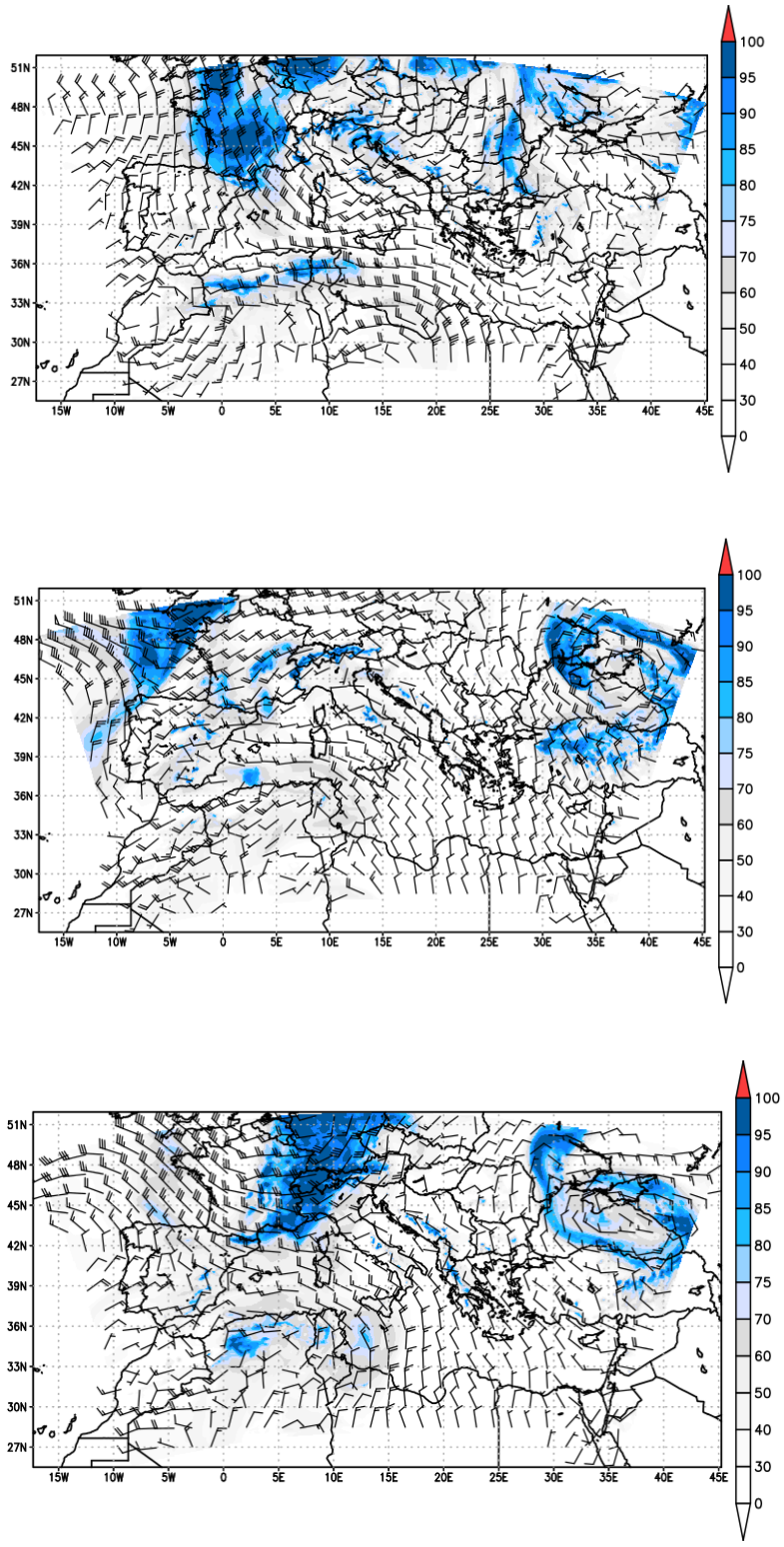

Figure S7. Vertical profiles of the potential temperature (green), water mixing ratio (w_{H2O}, blue), wind direction (purple) and wind speed (red). Data were corrected for STP using T= 20°C and P =1013.25 hPa. The water mixing ratio and wind speed are plotted using the upper horizontal axis. The top of the boundary layer Z_b and the wind shear level Z_s are indicated in line and in dashed line respectively. The height of Z_b was situated below the minimum flight level in F30 and F42. The height of Z_s was situated below the minimum flight level in F42.